Acta Crystallographica Section D
Biological Crystallography
ISSN 0907-4449

Structure of the D140N mutant of chitinase B from *Serratia marcescens* at 1.45 Å resolution

G. Kolstad,[a] B. Synstad,[a] V. G. H. Eijsink[a] and D. M. F. van Aalten[b]*

[a]Department of Chemistry and Biotechnology, Agricultural University of Norway, 1432 Ås, Norway, and [b]Wellcome Trust Biocentre, School of Life Sciences, University of Dundee, Dundee DD1 5EH, Scotland

Correspondence e-mail: dava@davapc1.bioch.dundee.ac.uk

Received 30 July 2001
Accepted 7 November 2001

PDB Reference: chitinase B D140N mutant, 1goi.

The crystal structure of the inactive D140N mutant of *Serratia marcescens* was refined to 1.45 Å resolution. The structure of the mutant was essentially identical to that of the wild type, with the exception of a rotation of Asp142 in the catalytic centre. In the mutant, this residue interacts with the catalytic acid (Glu144) and not with residue 140 as in the wild type. Thus, the 500-fold decrease in activity in the D140N mutant seems to be largely mediated by an effect on Asp142, confirming the crucial role of the latter residue in catalysis.

1. Introduction

Chitinase B (ChiB) from *S. marcescens* is a family 18 (Henrissat & Davies, 1997) two-domain exochitinase that degrades chitin chains from their non-reducing ends. The catalytic domain has a TIM-barrel fold in which β-strand 4 contains a characteristic D*x*D*x*E sequence motif that includes the catalytic glutamate (Glu144). The catalytic mechanism of family 18 chitinases is unusual in that the *N*-acetyl group of the sugar bound to the −1 subsite acts as a nucleophile during the first step of catalysis, which leads to the formation of an oxazolinium ion intermediate (Brameld & Goddard, 1998; Knapp *et al.*, 1996; Tews *et al.*, 1997; van Aalten *et al.*, 2001; Fig. 1). Mutation of Asp140 to asparagine (and the corresponding mutation in other family 18 chitinases) leads to a significant decrease in enzyme activity (∼500-fold; Synstad *et al.*, 2000; see also Tsujibo *et al.*, 1993; Watanabe *et al.*, 1993). Interestingly, Asp140 is located in the TIM-barrel core, relatively distant from the catalytic glutamate (the shortest distance between side chains atoms is 8.1 Å). In the wild-type enzyme, Asp142 points towards Asp140 and the two residues share a proton (van Aalten *et al.*, 2000; Fig. 1). It was recently shown that Asp142 rotates away from Asp140 towards Glu144 upon substrate binding (van Aalten *et al.*, 2001; Fig. 1). This rotation was suggested to play an essential role in 'cycling' of the pK_a of the catalytic acid during catalysis. It was also shown that the negative charge on Asp140 generated by the rotation of Asp142 is compensated for by adjustments in the core of the TIM-barrel which result in strengthening of hydrogen bonds between Asp140 and the conserved residues Ser93 and Tyr10 (van Aalten *et al.*, 2001).

The currently available results suggest a possible role for Asp140 during catalysis, but they do not readily explain the effect of the D140N mutation on catalytic activity. Since

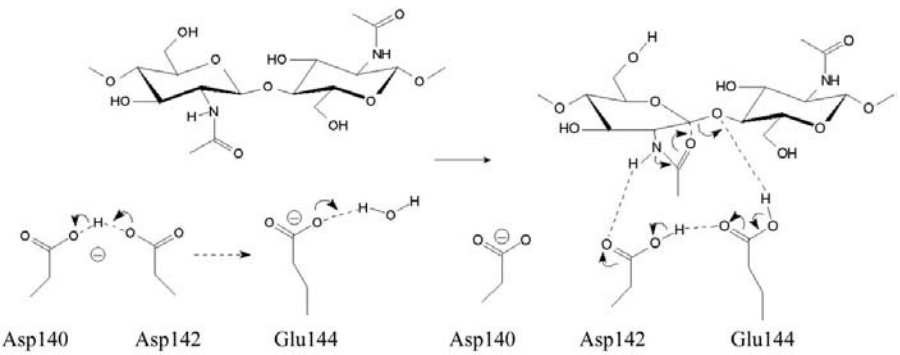

Figure 1
Initial steps during catalysis in family 18 chitinases (Brameld & Goddard, 1998; Tews *et al.*, 1997; van Aalten *et al.*, 2001). The dashed arrow indicates rotation of Asp142.

Asp140 interacts intimately with several residues in the core of the TIM-barrel, one cannot exclude that the mutational effect of the D140N mutation results from conformational changes in the enzyme. These issues were addressed by solving the crystal structure of the D140N mutant of chitinase B.

2. Experimental methods

2.1. Protein expression, purification and crystallization

Site-directed mutagenesis (using Stratagene's QuickChange kit) and the expression and purification of chitinase B variants have been described previously (Brurberg *et al.*, 1996; Synstad *et al.*, 2000). For crystallization, lyophilized protein was dissolved to 1 mg ml^{-1} in 20 m*M* Tris pH 8.5. The solution was dialyzed against the same buffer for 24 h at 277 K. After dialysis, the protein solution was concentrated to 10 mg ml^{-1} (using UltraFree-MC filter units from Millipore with 30 kDa cutoff) and used directly in hanging-drop vapour-diffusion crystallization experiments. Crystallization plates (Hampton Research) were set up with 1 ml well solutions made by combining three different buffers (citrate pH 6.0, HEPES pH 7.0 and Tris pH 8.0), glycerol, ammonium sulfate and dH_2O. Small crystals appeared after a few days in 10% glycerol, 1.25 *M* ammonium sulfate and 100 m*M* HEPES pH 7. After three months, the crystals had grown to approximate dimensions of 0.1 × 0.1 × 0.1 mm.

2.2. Data collection, solution and refinement

Diffraction data were collected at the European Synchrotron Radiation Facility, Grenoble (beamline ID14-1). All data were processed using *DENZO* and reflections were merged using *SCALEPACK* from the *HKL* suite (Otwinowski & Minor, 1997). A set of 1921 reflections was set aside for calculation of $R_{\rm free}$. Refinement was started using the previously solved ChiB structure as a phasing model. The initial stages of refinement were undertaken with *CNS* (Brunger *et al.*, 1998) and included simulated annealing. The final *CNS* model was then further refined in *SHELX*97 (Sheldrick, 1990) with individual anisotropic temperature factors. All refinement was supplemented with iterative model building in *O* (Jones *et al.*, 1991). Details of the refinement process and of the final model structure are shown in Tables 1 and 2.

3. Results and discussion

3.1. The structure

The structure of the D140N mutant of ChiB was refined to 1.45 Å resolution using synchrotron-radiation diffraction data (Tables 1 and 2). With 998 residues in the asymmetric unit, the structure is one of the few large structures to be solved at this high resolution (only four structures with more than 600 amino acids refined to a resolution higher than 1.45 Å had been deposited to the PDB as of July 2001). The overall structure of the D140N mutant was similar to that of the wild type (RMSD on catalytic domain C$^{\alpha}$ atoms is 0.12 Å). Analysis of the Ramachandran plot using *PROCHECK* (Laskowski *et al.*, 1993) showed 90.5% of the residues in most favoured regions, 9.4% in favoured regions, 0.1% in generously allowed regions and none in disallowed regions.

Table 1
Progress of refinement in *CNS* and *SHELX*-97.

	R	$R_{\rm free}$
Molecular-replacement solution (*CNS*)	26.69	28.45
Model building (*CNS*)	26.18	27.78
Model building, water molecules (*CNS*)	22.67	24.33
Conversion to *SHELX*-97	22.57	26.53
Anisotropic *B* factors (*SHELX*-97)	19.01	24.26
Model building, alternate conformations (*SHELX*-97)	19.00	23.92
Model building, glycerols, SO_4^{2-} (*SHELX*-97)	18.40	23.39
Model building, water molecules (*SHELX*-97)	17.17	22.76
Model building, water molecules (*SHELX*-97)	16.42	22.66
H atoms added to the refinement (*SHELX*-97)	15.94	21.78

Table 2
Refinement and structure-quality statistics.

Values in parentheses are for the outer shell. No resolution or σ cutoff was applied to the data used for refinement.

Data quality	
Resolution (Å)	17.0–1.45 (1.50–1.45)
$R_{\rm merge}$	0.037 (0.38)
No. reflections measured	600078
No. unique reflections	191634
Mean $I/\sigma(I)$	14.7 (2.7)
Completeness (%)	99.3 (99.5)
Redundancy	3.5
Crystal parameters	
Space group	$P2_12_12_1$
Unit-cell parameters (Å)	a = 55.90, b = 104.02, c = 186.52
Refinement	
No. of protein atoms	7998
No. of solvent waters	1016
No. of glycerol atoms	78
No. of SO_4^{2-} atoms	15
$R_{\rm cryst}$	0.164
$R_{\rm free}$	0.227
RMSD from bond ideality (Å)	0.017
RMSD from angle ideality (°)	2.32
Average main-chain B (Å^2)	21.7

The only notable changes in main-chain atoms concerned residues 301–302 and 487–488, all far from the catalytic centre. The high-resolution data of D140N allowed a precise determination of the structures of these residues, which had relatively high *B* factors in the wild-type structure. Water molecules observed in the core of the wild-type TIM-barrel (van Aalten *et al.*, 2000) were also found in the D140N structure. A superposition of D140N and the wild-type structure showed that the positions of the water molecules differed by at most 0.3 Å. Side-chain conformations were generally as in the wild-type structure, with the exception of a few surface-exposed charged residues (which is normal) and Asp142 which rotates 111° around χ_1 (Fig. 2). The wild type and the mutant are essentially identical with respect to the position of residue 140 and the surrounding hydrogen-bonding network. The rotation of Asp142 is similar to the rotation observed upon substrate binding (Fig. 2, van Aalten *et al.*, 2001) and is the only notable structural effect of the D140N mutation in the catalytic centre region.

Interestingly, the adjustments of Ser93 and Tyr10 that accompany rotation of Asp142 upon substrate binding in the wild-type enzyme are not observed in the D140N mutant (Fig. 2). From a structural point of view, the observed rotation of Asp142 towards Glu144 could be explained as follows. In the wild-type apoenzyme, Asp142 and Asp140 share a proton, with Asp142 contributing to the stabilization (dispersion) of the buried negative charge on Asp140 (Fig. 1). After removal of the charge at position 140 through mutation to the corresponding amide, the orientation of Asp142 towards Glu144 seems to be the more favourable as this brings the charged Asp142 closer to the solvent, allowing charge dispersion *via* the sharing of a proton with Glu144.

3.2. The role of Asp140 during catalysis

The D140N structure shows that the large decrease in activity upon the D140N mutation (Synstad *et al.*, 2000) is not a consequence of large conformational changes in the enzyme but arises from local effects. In the currently proposed catalytic mechanism for ChiB (Fig. 1), Glu144 becomes protonated upon substrate binding prior to rotation of Asp142. The rotation of protonated Asp142 towards Glu144 increases the acidity of the latter, which promotes proton transfer to the oxygen in the scissile glycosidic bond (van Aalten *et al.*, 2001 and references

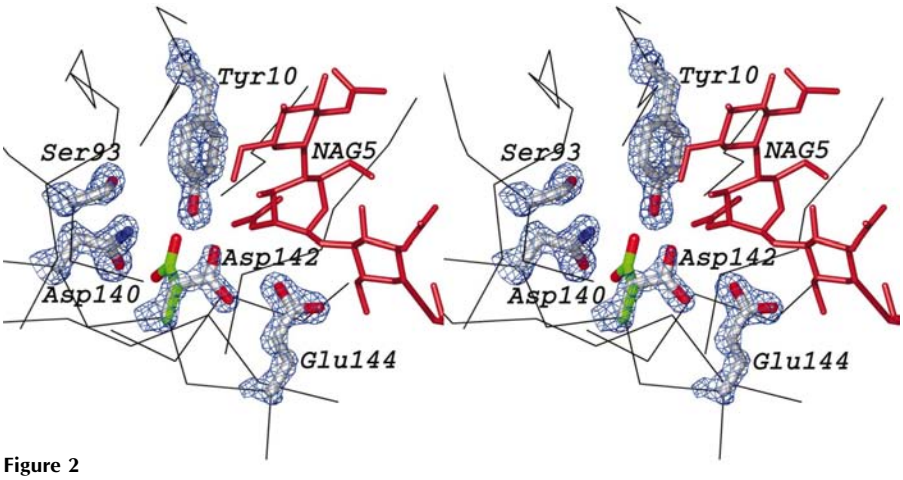

Figure 2
The D*x*D*x*E motif and the conserved residues Tyr10 and Ser93 in the ChiB D140N mutant structure (black backbone trace, side chains in stick representation). The location of the −2, −1, +1 sugar-binding subsites as observed in the complex with pentameric substrate (van Aalten *et al.*, 2001) is also shown (red stick model). In the ChiB apo structure, residue Asp142 points into the TIM barrel towards Asp140. This conformation is shown as a stick model with C atoms coloured green. The electron density (final ChiB-D140N $2|F_o| - |F_c|, \varphi_{calc}$ map) around the side chains is contoured at 2.25σ.

therein). In principle, it would seem that Asp142 in the D140N mutant can still play this role. However, it is possible that the rotation of Asp142 needs to take place concurrently with substrate binding, since this binding involves distortion of the −1 sugar in which the rotating Asp142 plays a key role (Fig. 1; Tews *et al.*, 1997; Brameld & Goddard, 1998; van Aalten *et al.*, 2001). Although not directly visible in the structures, it is possible that the concomitant adjustments of Ser93 and Tyr10 (which do not occur in the D140N structure) also contribute to establishing productive substrate binding.

Another explanation for the reduced activity of the D140N mutant could be that the interaction of Asp142 with Glu144 prevents Glu144 from being protonated at all in the enzyme–substrate complex, which would decrease catalytic efficiency.

4. Conclusions

The essential role of Asp140 for catalysis in chitinase B from *S. marcescens* seems to be primarily mediated through its effects on the conformation of Asp142. The changed conformation of Asp142 is likely to affect the protonation state of the catalytic acid, as well as the ability to bind substrate in a productive manner.

We thank the ESRF, Grenoble for the time at beamline ID14-1. We thank Jens E. Nielsen for helpful dicussions on protein electrostatics. This work was supported in part by the European Union, grant No. BIO4-CT-960670, by a grant from the Norwegian Research Council to BS and by a Wellcome Trust Career Development Research Fellowship to DMFvA.

References

Aalten, D. M. F. van, Komander, D., Synstad, B., Gåseidnes, S., Peter, M. G. & Eijsink, V. G. H. (2001). *Proc. Natl Acad. Sci. USA*, **98**, 8979–8984.
Aalten, D. M. F. van, Synstad, B., Brurberg, M. B., Hough, E., Riize, B. W., Eijsink, V. G. H. & Wierenga, R. K. (2000). *Proc. Natl Acad. Sci. USA*, **97**, 5842–5847.
Brameld, K. A. & Goddard, W. A. (1998). *J. Am. Chem. Soc.* **120**, 3571–3580.
Brunger, A. T., Adams, P. D., Clore, G. M., DeLano, W. L., Gros, P., Grosse-Kunstleve, R. W., Jiang, J. S., Kuszewski, J., Nilges, M., Pannu, N. S., Read, R. J., Rice, L. M., Simonson, T. & Warren, G. L. (1998). *Acta Cryst.* D**54**, 905–921.
Brurberg, M. B., Nes, I. F. & Eijsink, V. G. H. (1996). *Microbiology*, **142**, 1581–1589.
Henrissat, B. & Davies, G. (1997). *Curr. Opin. Struct. Biol.* **7**, 637–644.
Jones, T. A., Zou, J. Y., Cowan, S. W. & Kjeldgaard, M. (1991). *Acta Cryst.* A**47**, 110–119.
Knapp, S., Vocadlo, D., Gao, Z. N., Kirk, B., Lou, J. P. & Withers, S. G. (1996). *J. Am. Chem. Soc.* **118**, 6804–6805.
Laskowski, R. A., MacArthur, M. W., Moss, D. S. & Thornton, J. M. (1993). *J. Appl. Cryst.* **26**, 283–291.
Otwinowski, Z. & Minor, W. (1997). *Methods Enzymol.* **276**, 307–326.
Sheldrick, G. M. (1990). *Acta Cryst.* A**46**, 467–473.
Synstad, B., Gåseidnes, S., Vriend, G., Nielsen, J.-E. & Eijsink, V. G. H. (2000). *Adv. Chitin Sci.* **4**, 524–529.
Tews, I., van Scheltinga, A. C. T., Perrakis, A., Wilson, K. S. & Dijkstra, B. W. (1997). *J. Am. Chem. Soc.* **119**, 7954–7959.
Tsujibo, H., Orikoshi, H., Imada, C., Okami, Y., Miyamoto, K. & Inamori, Y. (1993). *Biosci. Biotechnol. Biochem.* **57**, 1396–1397.
Watanabe, T., Kobori, K., Miyashita, K., Fujii, T., Sakai, H., Uchida, M. & Tanaka, H. (1993). *J. Biol. Chem.* **268**, 18567–18572.